IJE TRANSACTIONS B: Application Vol. 27, No. 8, (August 2014) 1307-1316

International Journal of Engineering

Journal Homepage: www.ije.ir

Experimental and Numerical Studies on the Energy Absorption Characteristics of Simple and Multi-cell Shapes of Quasi-hemisphere Thin-walled Structures

M. Parsapour

Mechanical Engineering Department, Bu-Ali Sina University, Hamedan, Iran

PAPER INFO

Paper history:
Received 19 January 2014
Received in revised form 25 February 2014
Accepted 06 March 2014

Keywords:
Thin-walled Structure
Energy Absorber
Quasi-hemisphere
Multi-cell.

ABSTRACT

Energy absorbers are used to reduce accident induced damages. Thin-walled energy absorbers are widely used in modern industries due to their high efficiency and ease of manufacturing. In this study, thin-walled stainless steel structures in quasi-hemisphere geometry were subjected under quasi-static loading using Santam 150KN apparatus. Experimental results were compared with the results of numerical simulations by LS-DYNA and it was shown that there is a good agreement between experimental and numerical results. Two different collapse types in radial and circumferential directions were observed. Also, the multi-cell quasi-hemisphere specimens from 3 to 6 cells were numerically investigated and it is observedthat increasing the number of cells increases the absorbed energy. Increasing the thickness of the quasi-hemisphere sample in smaller diameter specimens is more effective. The results showed that Six-cell specimen with the largest diameter and the minimum thickness has the most increase of Specific Absorbed Energy (SAE) with respect to simple section.

doi: 10.5829/idosi.ije.2014.27.08b.17

1. INTRODUCTION

Safety for vehicles has long been regarded by designers. One of the most important safety issues in designing of vehicle is minimizing loss of lives and damages in collisions. To avoid these losses, energy absorbers are used. These structures dissipate crash energy in the form of plastic deformation and protect sensitive regions such as passenger's cabin. Thin-walled structures are used because of low weight, low production cost and ease of manufacturing. The primary geometries for the section of these structures are circle, square, triangle, polygon and conical which are used in hollow or foam-filled cases.

Main parameters in energy-absorbing structures are the MCL (Mean Crushing Load) and SAE (Specific Absorbed Energy). Thin-walled circular tubes under axial loading were first studied theoretically by Alexander [1]. Folding mechanism of thin-walled tubes was introduced as a mechanism for absorbing energy. Experimental and theoretical investigations on the behavior of circular and square sections in quasi- static and dynamic conditions were carried out by Abramowicz and Wierzbicki [2, 3], Abramowicz and Jones [4, 5] and Andrews et al. [6]. Experimental studies of Abramowicz and Jones on steel square tubes showed that crushing will occur in both symmetric and asymmetric modes. Langseth and Hopperstad [7] performed static and dynamic tests on the square samples of aluminum and showed that the MCL in the dynamic mode is more than the static one. mechanical behavior of circular, square, tapered and conical thin-walled sections have been compared both numerically and experimentally. In the past two decades, square sections in multi-cell mode have been studied by researchers. Chen and Wierzbicki [8] presented analytical equations for predicting the MCL of square tubes in simple, two-cells (2 × 1) and three cells (3 × 1) cases using the SFE theory. Heung-Soo Kim [9] investigated the behavior of thin-walled square tubes both numerically and theoretically. He showed that

*Coresponding Author's Email: m.parsapour@basu.ac.ir (M. Parsapour)

Please cite this article as: M. Parsapour, Experimental and Numerical Studies on the Energy Absorption Characteristics of Simple and Multi-cell Shapes of Quasi-hemisphere Thin-walled Structures. International Journal of Engineering (IJE) Transactions B: Applications Vol. 27, No. 8, (2014): 1307-1316

adding elements at the corners of the square cross section increases SAE up to 1.9 times. Zhang et al. [10] studied the multi-cell square sections of the equal cell size both numerically and theoretically and showed that the square section in the case of 3×3 increases absorbed energy by 100% compared with the simple square section. Their proposed sections contained equal sized and right angle cells. Multi-cell square sections with equal and unequal cell sizes were studied by Alavi Nia and Parsapour [11] both experimentally and numerically. Furthermore, they examined the non-equal cell size square sections theoretically and numerically and showed that smaller cells at the corners of the section increase the ability to absorb energy. They also studied thin-walled multi-cell shape of square, triangular and polygonal sections and investigated two types of multi-cell shapes. They reported that perpendicular multi-cell element increase SAE more than other types [12]. Cylindrical multi-cell sections studied numerically by Tang et al. [13]; they showed that cylindrical sections with two radial blade have more capability of energy absorption than other models with the same weight.

Shariati and Allahbakhsh [14] carried out an experimental and numerical study on the behavior of semi-spherical specimens under quasi-static loading with different compressive jaws. They also investigated the effects of thickness and diameter of samples on the energy absorption characteristics. Gupta et al. studied Buckling modes of spherical thin-walled tubes experimentally and numerically under axial loads. They also studied the behavior of shells under axial compression based on the formation of rolling and stationary plastic hinges [15].

Researches of thin-walled multi-cell tubes mostly were about square, circle and polygon geometries. The presented paper investigated the behavior of quasi-hemisphere thin-walled structures with shapes of simple and multi-cell. Samples were made from steel with a thickness of 0.3 mm and experiments have been done by Santam 150KN apparatus. Then, the behavior of the multicellular samples was examined using the LS-DYNA software. It was done after observation of acceptable agreement between numerical data and experimental results of quasi-hemisphere samples.

2. SPECIFICATION OF SPECIMENS

In this research, quasi-hemisphere samples in three diameters have been tested experimentally. The specimens were made from 0.3 mm thick steel sheet. Stainless steel material was used for fabrication of the samples because of better folding without any fracture in lower thicknesses. During loading, specimens collapsed without any crack or fracture and all folds had a regular pattern. Mechanical properties of the material obtained via ASTM E8M Standard tension test [16] are listed in Table 1. This table shows the average values of parameters obtained for three tension test samples.

2. 1. Number of Samples and Their Codes

The codes of Sp are used for quasi-hemisphere specimens. Specimens are made in three sizes, small, medium and large and are specified with the letters s, m and l, respectively. Three, and in some cases four samples were made for each case. The number at the end of each code represents the number of specimens in each type. Table 2 shows the code of tested specimens. Dimensions of the specimens are shown in Figure 1 and Table 3. The fabricated experimental samples are illustrated in Figure 2.

TABLE 1. Mechanical properties of samples

Property	Symbol	Value
Young's modulus	E	202 GPa
Yield stress	σ_y	420 MPa
Ultimate stress	σ_u	560 MPa

TABLE 2. Codes of experimental samples.

Number of sample	Small	Medium	Large
First	Sp-s-1	Sp-m-1	Sp-l-1
Second	Sp-s-2	Sp-m-2	Sp-l-2
Third	Sp-s-3	Sp-m-3	Sp-l-3
Forth	Sp-s-4	Sp-m-4	-

TABLE 3. Dimension of experimental samples. (Dimensions are in millimeter.)

Specimen	D	d	h
Sp-s	105	55	40
Sp-m	160	90	50
Sp-l	170	95	55

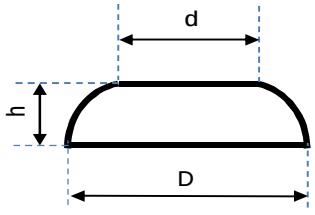

Figure 1. Quasi-hemisphere.

Figure 2. Sp-l, Sp-m and Sp-s (left to right)

Figure 3. Santam 150KN apparatus.

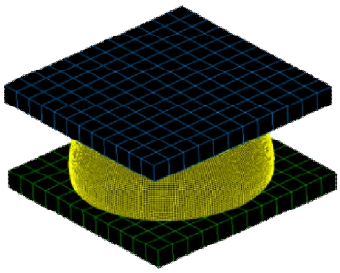

Figure 4. Finite element model of the quasi-hemisphere and jaws.

3. EXPERIMENTAL TESTS

Axial quasi-static loading of the specimens was carried out by Santam 150KN apparatus. This device has two jaws; the lower jaw is fixed and the upper jaw moves in a vertical direction. Samples were placed between the jaws and compressed by the movable jaw. Loading rate for all samples was 10 mm/min. In compressing square, circular or polygonal tubes, using constraints in order to prevent slippage is needed and in some cases is essential. Furthermore, different shapes of trigger are used for square tubes to reduce the initial peak load and obtaining regular folding pattern. Quasi-hemisphere specimen due to its geometrical specification does not need any constraint or trigger. Quasi-hemisphere specimens were tested in this investigation without any constraints for fixing or any trigger for initiating the folding. No slippage was observed during loading. The Santam device is shown in Figure 3.

4. NUMERICAL SIMULATIONS

The development of nonlinear finite element code like LS-DYNA made it possible to analyze structures under static and impact loads. There are different element models inside the library of the software which have mostly been developed by Hughes [17, 18] and Belytschko et al. [19]. Their aim was to correct the problem of zero energy and also improvement of computational efficiency. Axial compression loading of the tested samples was simulated by nonlinear explicit FE code LS-DYNA. Shell element was applied in simulation of tubes due to their similar behavior as in experimental test. The two jaws are not deformed during loading test. Therefore, they were considered as rigid jaws. Solid element with rigid material model was used to simulate the jaws. In quasi-static simulation the tube was held at the lower jaw and an incremental displacement was applied by upper jaw in vertical downward. Simulations with different mesh size were performed to find a suitable element size for the tubes. Absorbed energy trend by different mesh size became stable at the element size of 2mm. The total number of elements for a simple quasi-hemisphere tube was obtained to be about 20000. Because of larger size and more walls of other tubes, their total numbers are greater and reach as high as 40000. Further examinations showed that energy absorption can be estimated by using only three integration points (NIP=3) through the shell thickness. Also, zero energy deformation or hourglass energy [19-21] was checked. In dynamic simulation as in impact loading, the effects of high velocity should be considered and the material model should include the strain rate. Due to low velocity in quasi-static loading, the strain rate is neglected and we can use a model like piecewise linear plasticity which can show plastic deformations as needed in our investigation. There are many researches in which piecewise linear plasticity material model has been used for energy absorber tubes and good agreement between numerical and experimental results has been reported [8, 11, 12, 22, 23]. It is indispensable to define contact mode to prevent element penetration. Firstly, automatic surface to surface contact was chosen between the tube and jaws. During loading process, tube wall collide with itself indicating that a contact mode should be considered. Contact automatic single surface was applied for the tubes. The contact friction coefficient was set at 0.3 to prevent slippage due to numerical error between the two surfaces. The finite element model of the process is shown in Figure 4.

5. RESULTS AND DISCUSSIONS

5. 1. The Simple Quasi-hemisphere Deformation modes of the tested (right) and simulated (left) specimens after loading are shown in Figure 5. For better illustration of the folds, displacement contour in the perpendicular direction to the loading axis was used. As Figure 5 shows, there is a good agreement between deformation modes of the tested and simulated results. Bottom views of quasi-hemispheres are shown in Figure 6 for better observation of folding. During loading, at first, collapses in radial direction start then collapses in circumferential direction appear. Both folding modes are shown in Figure 6.

Load-displacement curves of quasi-hemisphere specimens, obtained from experiments are shown in Figure 7. As can be seen, the curves related to the small samples Sp-s has a maximum value. Also, due to a lower height of these types, their crushing length is smaller than those of the Sp-m and Sp-l samples.

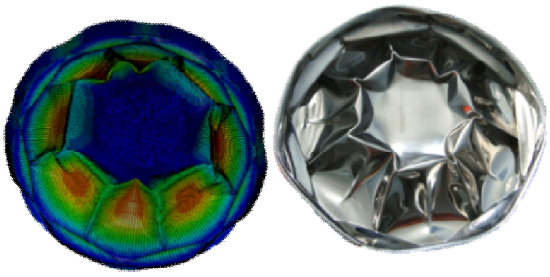

(a)

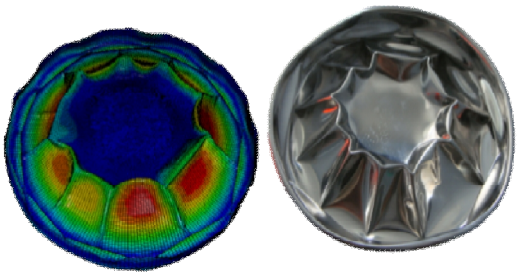

(b)

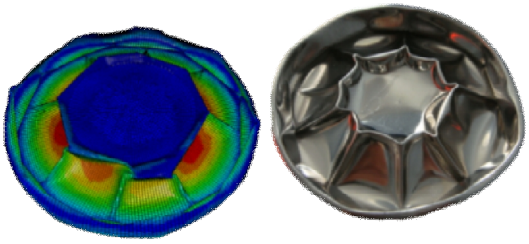

(c)

Figure 5. Bottom view of (a) Sp-l, (b) Sp-m and (c) Sp-s. after loading by simulation and experiment.

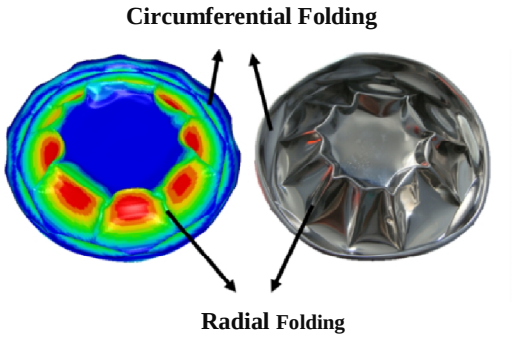

Figure 6. Collapse modes of quasi-hemisphere, numerical (left) and experiment (right).

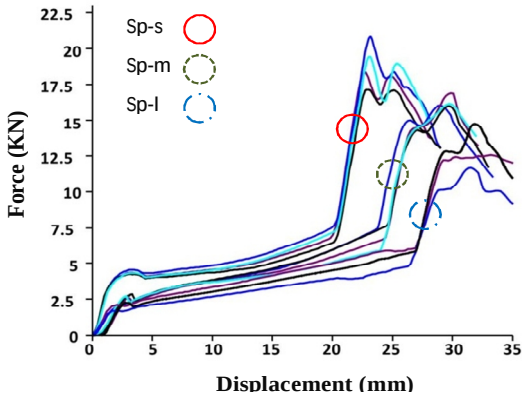

Figure 7. Force-Displacement curves of quasi-hemispherical specimens (experiment).

This trend is also true for Sp-m samples compared with samples Sp-l. Notable point in this figure is the changes in rising trend of load. Initially, there is a maximum value (peak) which is due to folds that occur in the radial direction. Increasing trend of energy absorption continues with a low slope till crushing lengths of approximately 20, 25 and 30 mm, for samples Sp-s, Sp-m and Sp-l, respectively. After that, a dramatic rise is observed which is referred to the folding in the circumferential direction. Load-displacement curves from experiment and numerical simulations for Sp-s, Sp-m and Sp-l specimens are shown in Figure 8. This figure depicts an acceptable agreement between the tests data and simulation results. Table 4 shows the values of MCL and CFE (Crush Force Efficiency) for quasi-hemisphere specimens obtained from experiment and simulation. Equation (1) shows the calculation of CFE.

$$CFE = 100 \times \frac{Mean\ Load}{Peak\ Load} \quad (1)$$

Samples with lower level of CFE need more force to initiate folding which is not desirable.

In other tubes with square or circular geometry, a

large amount of force is needed at the first step of loading which indicated that these tubes cannot absorb energy when the force level is lower than peak load and even when it is almost equal to the mean crush load. Quasi-hemisphere tubes have this considerable point that they do not need a large load for the first step of deformation. In Table 4, the MCL rows specified with the numbers 1 to 4 indicate the number of samples that have been tested. In order to better compare the results, average values of MCL are given with "Average of MCL".

According to Table 4, a good agreement is observed between experimental results and numerical simulations. From Table 4, it can be seen that the MCL for quasi-hemisphere specimens at small sample of Sp-s is more than two others. CFE Values of specimens are almost identical, and the differences are negligible.

TABLE 4. Results of experimental tests and simulation of specimens

Specification	Sp-s	Sp-m	Sp-l
MCL-1 (KN)	8.4	6.3	4.9
MCL-2 (KN)	7.5	6.6	5.78
MCL-3 (KN)	7.85	6.2	6
MCL-4 (KN)	7.72	6.6	-
Average of MCL (KN)	7.86	6.425	5.56
CFE (Test)	43	42	46
MCL-FE (KN)	7.2	6.17	5.7
CFE (FEM)	48	44	38

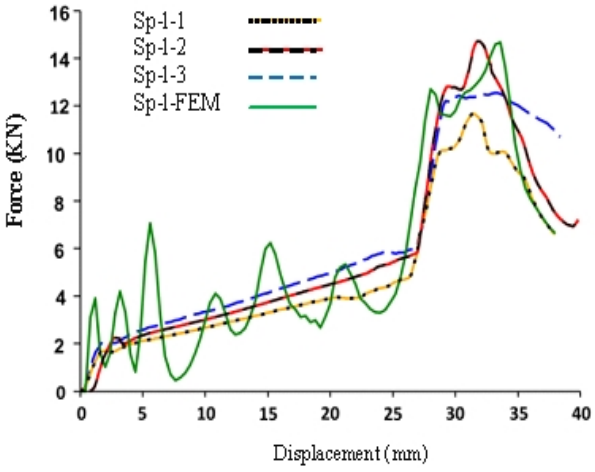

(a)

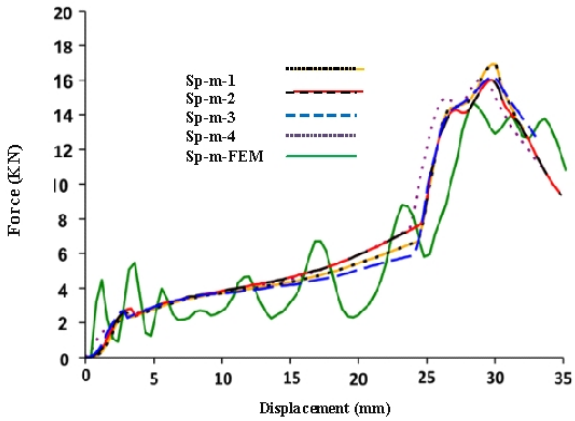

(b)

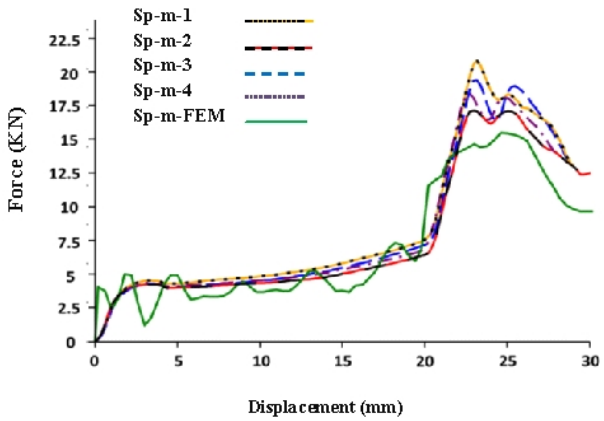

(c)

Figure 8. Force-displacement curves of specimens in tests and simulations (a) Sp-l, (b) Sp-m and (c) Sp-s.

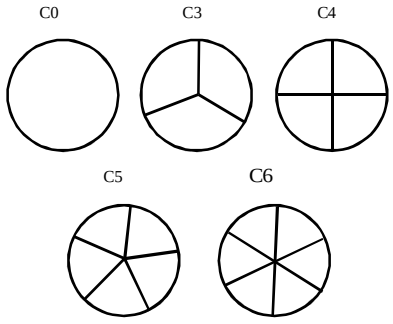

Figure 9. Multi-cell modes of quasi-hemispherical specimens.

5. 2. The Multi-Cell Quasi-hemisphere Multi-cell quasi-hemisphere specimens have also been studied in this investigation by numerical simulations. In this section, ordinary specimens (single cell) are specified with code C0 and 3 to 6 cell multi-cell specimens were named with the codes C3 to C6. Letter C represents cell and number after it indicates the number of cells. Placement of cells, for quasi-hemisphere specimens is

shown in Figure 9. Finite element three-cell quasi-hemisphere specimen is shown in Figure 10.

Simulations for four thicknesses of 0.3, 0.6, 0.9 and 1.2 mm and four diameters of 100, 130, 160 and 190 mm were done. Multi cellular elements prevent big collapses in radial direction and change them to small and more folds. The deformed shapes of multi-cell quasi-hemispherical specimens are shown in Figure 11. Absorbed energy versus bigger diameter to height ratio, D/h, for four thicknesses, absorbed energy versus the thickness for four D/h values and finally, energy absorption versus number of cells for the four D/h of the quasi-hemisphere specimens are shown in Figures 12-14, respectively. Figure 12 shows that an increase in the ratio D/h of the quasi-hemisphere with code C0 in all four thicknesses reduces the absorbed energy, while greater values of D/h in multi-cell specimens, had a positive impact on increase of absorbed energy. The positive impact of increased thickness on absorbed energy is shown in Figure 13. For each of four sizes of the simple and multi-cell specimens, increase in thickness results more absorbed energy. According to Figure 14, multi-cell elements increase energy absorption in four sizes and four thicknesses.

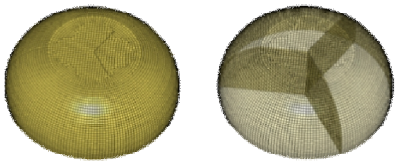

Figure 10. Quasi-hemisphere in Multi-cell shape with Three cells.

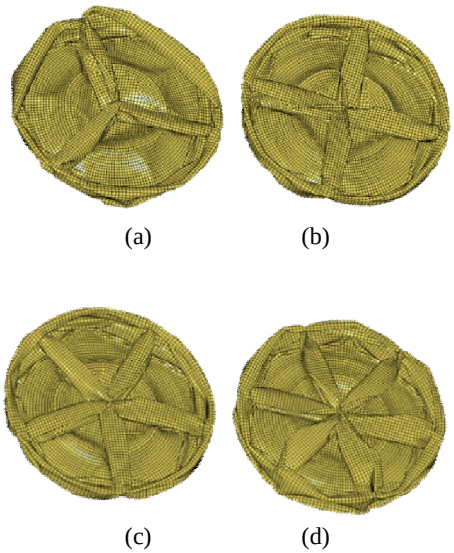

(a) (b)

(c) (d)

Figure 11. Bottom view of multi-cell quasi-hemispherical samples after loading by numerical simulation: a) 3 cells, b) 4 cells, c) 5 cells and d) 6 cells.

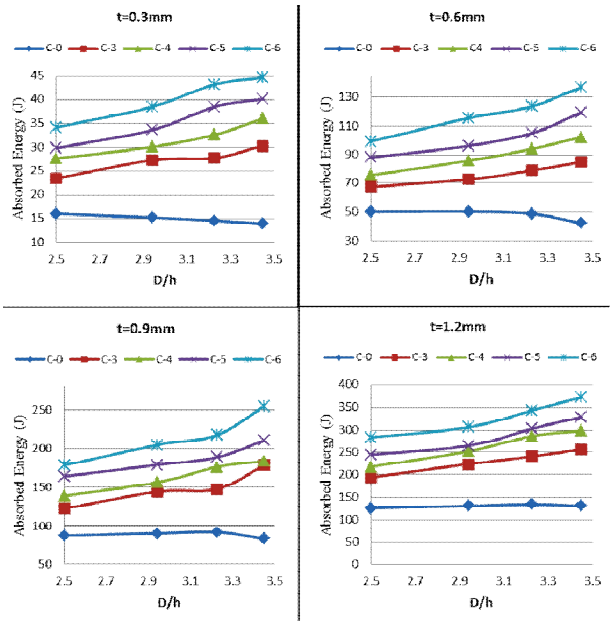

Figure 12. Absorbed energy-D/h curves in different cell numbers and thicknesses.

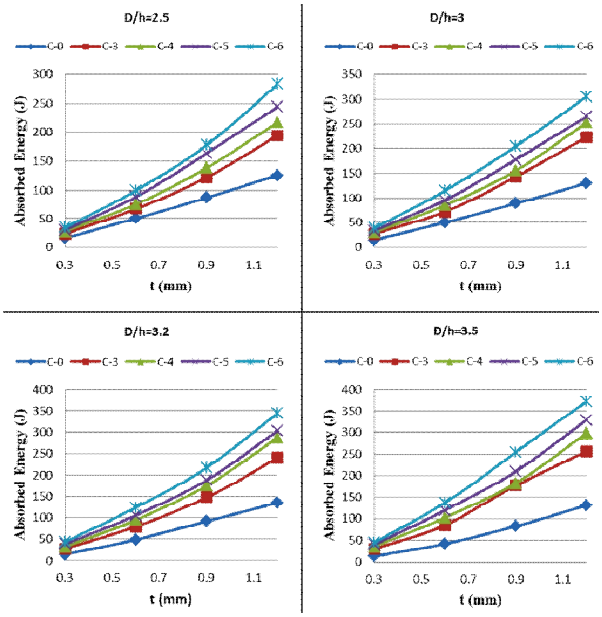

Figure 13. Absorbed energy-thickness curves in different cell numbers and D/h.

The absorbed energy per unit mass of the samples, SAE, is given in Table 5. As can be seen, the highest value of SAE among the specimens belongs to the Sp-D100-C6 sample. The number after the letter D represents the diameter of the largest section and the number after letter C is the number of cells. According to this table, six-cell specimens have the highest energy absorption.

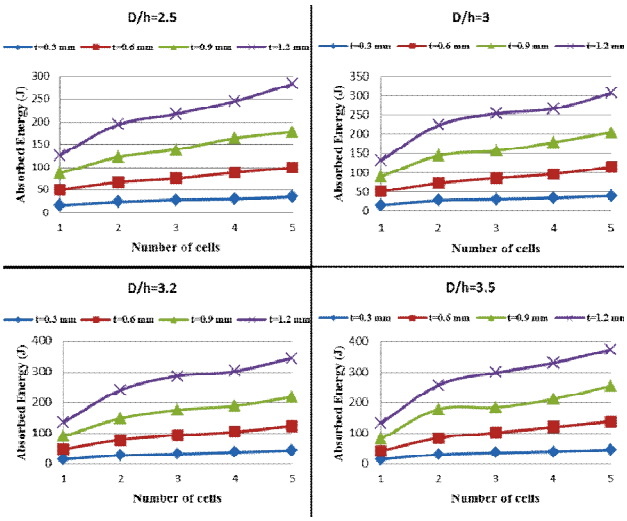

Figure 14. Absorbed energy-number of cells curves in different D/h and thicknesses.

The increase in absorbed energy for multi-cell specimens compared to the simple specimen with code C0, with the same diameter and thickness, is shown in Figure 15. Among the specimens, the largest increase of the absorbed energy belongs to specimen Sp-D190-C6.

For sample Sp-D100 (lowest diameter) the greatest effect of increase in number of cells on absorbed energy is observed for the thicknesses of 0.9 and 1.2 mm, while for the sample Sp-D190 (highest diameter), this phenomenon occurs in thicknesses of 0.3 and 0.6. It shows that increasing the thickness of the quasi-hemisphere sample in smaller diameter is more effective.

TABLE 5. SAE results of specimens.

Specimen Code	h (mm)	D (mm)	D/h	SAE(J/gr) at t=0.3mm	SAE(J/gr) at t=0.6mm	SAE(J/gr) at t=0.9mm	SAE(J/gr) at t=1.2mm
Sp-D100-C0	40	100	2.5	0.45	0.7	0.81	0.88
Sp-D100-C3	40	100	2.5	0.49	0.7	0.85	1.02
Sp-D100-C4	40	100	2.5	0.53	0.73	0.89	1.05
Sp-D100-C5	40	100	2.5	0.53	0.79	0.98	1.1
Sp-D100-C6	40	100	2.5	0.57	0.83	1	1.2
Sp-D130-C0	45	130	2.8	0.27	0.46	0.54	0.6
Sp-D130-C3	45	130	2.8	0.38	0.6	0.69	0.77
Sp-D130-C4	45	130	2.8	0.38	0.55	0.65	0.81
Sp-D130-C5	45	130	2.8	0.4	0.57	0.71	0.79
Sp-D130-C6	45	130	2.8	0.43	0.64	0.76	0.85
Sp-D160-C0	50	160	3.2	0.18	0.31	0.4	0.43
Sp-D160-C3	50	160	3.2	0.27	0.4	0.48	0.6
Sp-D160-C4	50	160	3.2	0.3	0.43	0.53	0.65
Sp-D160-C5	50	160	3.2	0.33	0.45	0.53	0.65
Sp-D160-C6	50	160	3.2	0.34	0.5	0.58	0.68
Sp-D190-C0	55	190	3.5	0.13	0.2	0.26	0.31
Sp-D190-C3	55	190	3.5	0.22	0.31	0.44	0.47
Sp-D190-C4	55	190	3.5	0.25	0.35	0.42	0.5
Sp-D190-C5	55	190	3.5	0.26	0.38	0.45	0.53
Sp-D190-C6	55	190	3.5	0. 27	0.4	0.51	0.56

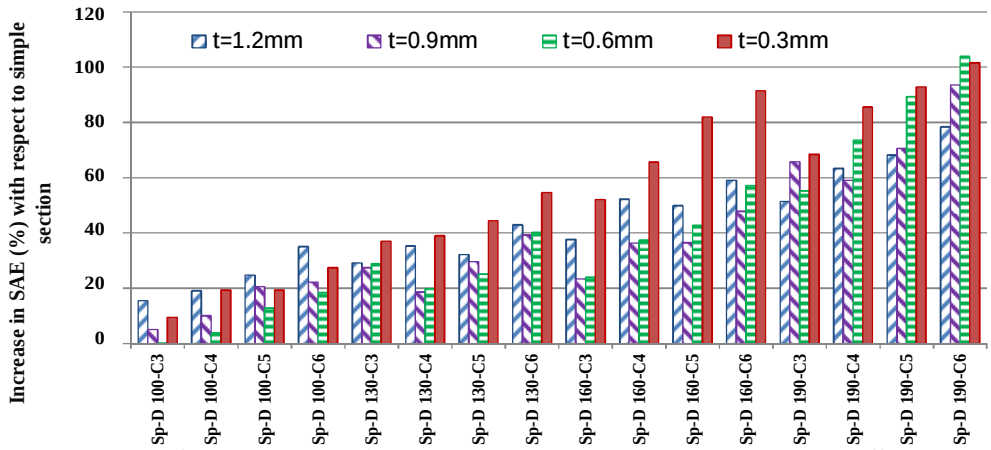

Figure 15. Percentage of increase in SAE of specimens with respect to their simple section in different thicknesses

6. CONCLUSION

In this paper, the mechanical behavior of quasi-hemisphere thin-walled structures under quasi-static load was studied by experimental tests. The same samples were investigated by numerical simulation with LS-DYNA software and acceptable agreement was found between experimental data and numerical results. Also, numerical investigation was carried out for the samples in multi-cell state with 3 to 6 cells, for 4 different thicknesses and diameters. The results showed that increasing the number of cells increases the amount of absorbed energy. Increasing the thickness of the quasi-hemisphere sample in smaller diameter is more effective. Six-cell specimen with the largest diameter and the minimum thickness showed the most increase of SAE compared to the simple specimen.

7. REFERENCES

1. Alexander, J., "An approximate analysis of the collapse of thin cylindrical shells under axial loading", ***The Quarterly Journal of Mechanics and Applied Mathematics***, Vol. 13, No. 1, (1960), 10-15.
2. Wierzbicki, T. and Abramowicz, W., "On the crushing mechanics of thin-walled structures", ***Journal of Applied mechanics***, Vol. 50, No. 4a, (1983), 727-734.
3. Abramowicz, W. and Wierzbicki, T., "Axial crushing of multi-corner sheet metal columns", ***Applied Mechanics-Transactions ASME***, Vol. 56, No., (1989), 113-120.
4. Abramowicz, W. and Jones, N., "Dynamic axial crushing of square tubes", ***International Journal of Impact Engineering***, Vol. 2, No. 2, (1984), 179-208.
5. Abramowicz, W. and Jones, N., "Dynamic progressive buckling of circular and square tubes", ***International Journal of Impact Engineering***, Vol. 4, No. 4, (1986), 243-270.
6. Andrews, K., England, G. and Ghani, E., "Classification of the axial collapse of cylindrical tubes under quasi-static loading", ***International Journal of Mechanical Sciences***, Vol. 25, No. 9, (1983), 687-696.
7. Langseth, M. and Hopperstad, O., "Static and dynamic axial crushing of square thin-walled aluminium extrusions", ***International Journal of Impact Engineering***, Vol. 18, No. 7, (1996), 949-968.
8. Chen, W. and Wierzbicki, T., "Relative merits of single-cell, multi-cell and foam-filled thin-walled structures in energy absorption", ***Thin-Walled Structures***, Vol. 39, No. 4, (2001), 287-306.
9. Kim, H.-S., "New extruded multi-cell aluminum profile for maximum crash energy absorption and weight efficiency", ***Thin-Walled Structures***, Vol. 40, No. 4, (2002), 311-327.
10. Zhang, X., Cheng, G. and Zhang, H., "Theoretical prediction and numerical simulation of multi-cell square thin-walled structures", ***Thin-Walled Structures***, Vol. 44, No. 11, (2006), 1185-1191.
11. Alavi Nia, A. and Parsapour, M., "An investigation on the energy absorption characteristics of multi-cell square tubes", ***Thin-Walled Structures***, Vol. 68, (2013), 26-34.
12. Alavi Nia, A. and Parsapour, M., "Comparative analysis of energy absorption capacity of simple and multi-cell thin-walled tubes with triangular, square, hexagonal and octagonal sections", ***Thin-Walled Structures***, Vol. 74, (2014), 155-165.
13. Tang, Z., Liu, S. and Zhang, Z., "Analysis of energy absorption characteristics of cylindrical multi-cell columns", ***Thin-Walled Structures***, Vol. 62, (2013), 75-84.
14. Shariati, M. and Allahbakhsh, H., "Numerical and experimental investigations on the buckling of steel semi-spherical shells under various loadings", ***Thin-Walled Structures***, Vol. 48, No. 8, (2010), 620-628.
15. Gupta, N., Mohamed Sheriff, N. and Velmurugan, R., "Experimental and theoretical studies on buckling of thin spherical shells under axial loads", ***International Journal of Mechanical Sciences***, Vol. 50, No. 3, (2008), 422-432.
16. Standard, A., "E8," standard test methods for tension testing of metallic materials", ***Annual book of ASTM standards***, Vol. 3, (2004), 57-72.
17. Hughes, T., "Nonlinear dynamic finite element analysis of shells, nonlinear finite element analysis in structural mechanics", In: Proceedings of the Europe- U.S. workshop, Ruhr-University Bochum, Germany, (1981), 151-168.

18. Hughes, T.J., "The finite element method: Linear static and dynamic finite element analysis, Courier Dover Publications, (2012).
19. Belytschko, T., Liu, W.K. and Moran, B., "Nonlinear finite elements for continua and structures. ", ***Chichester, New York, John Wiley***, Vol. 16, No. 650. (2000)
20. Hallquist, J., "Ls-dyna theoretical manual", ***Livermore Software Technology Corporation***, . (1998)
21. LS-DYNA keyword user's, L., "Manual, version 970", ***Livermore Software Technology Corporation***, (2003).
22. Zhang, X. and Zhang, H., "Numerical and theoretical studies on energy absorption of three-panel angle elements", ***International Journal of Impact Engineering***, Vol. 46, (2012), 23-40.
23. Najafi, A. and Rais-Rohani, M., "Mechanics of axial plastic collapse in multi-cell, multi-corner crush tubes", ***Thin-Walled Structures***, Vol. 49, No. 1, (2011), 1-12.

Experimental and Numerical Studies on the Energy Absorption Characteristics of Simple and Multi-cell Shapes of Quasi-hemisphere Thin-walled Structures

M. Parsapour

Mechanical Engineering Department, Bu-Ali Sina University, Hamedan, Iran

PAPER INFO

Paper history:
Received 19 January 2014
Received in revised form 25 February 2014
Accepted 06 March 2014

Keywords:
Thin-walled Structure
Energy Absorber
Quasi-hemisphere
Multi-cell.

چکیده

از جاذب های انرژی به منظور کاهش صدمات ناشی از تصادفات استفاده می شود. جاذب‌های انرژی جدارنازک به دلیل کارایی بالا و سادگی تولید به طور گسترده‌ای در صنایع پیشرفته به کار می‌روند. در این بررسی، سازه‌هایی از جنس فولاد زنگ‌نزن به شکل شبه نیم‌کره به صورت شبه‌استاتیکی توسط دستگاه سنتام 150 KN بارگذاری شدند. نتایج تجربی با نتایج حاصل از شبیه‌سازی عددی مقایسه شدند و نشان داده شد که تطابق خوبی بین آن ها وجود دارد. دو نوع چین-خوردگی در جهت شعاعی و محیطی مشاهده شد. همچنین نمونه‌های چندسلولی شبه نیم‌کره مورد بررسی عددی قرار گرفت و نشان داده شد که افزایش سلول ها سبب افزایش انرژی جذب شده می‌گردد. افزایش ضخامت نمونه‌های شبه نیم‌کره در قطرهای کوچک تاثیر بیشتری دارد. نتایج نشان داد که نمونه شش سلولی با بیشترین قطر و کمترین ضخامت دارای بیشترین مقدار انرژی جذب شده مخصوص نسبت به مقطع ساده می‌باشد.

doi: *10.5829/idosi.ije.2014.27.08b.17*